IMPROVEMENT OF INTERLAMINAR STRENGTH ON CFRP LAMINATES BY CARBON FIBER STITCHING

Yutaka Iwahori, Takashi Ishikawa

Advanced Composite Evaluation Center
Institute of Space Technology and Aeronautics
Japan Aerospace Exploration Agency

Keywords: *Stitching, DCB, CAI, OHC, DNS*

Abstract

Stitching using carbon fiber (CF) thread for CFRP laminates have been investigated experimentally. The laminate is fabricated by using low cost in-plane carbon fiber (TORAY T-700GC), special carbon fiber stitch thread (Mitsubishi Rayon TR-40 1K) and epoxy resin (TORAY TR-A31) for RTM. This CF stitched CFRP laminates are manufactured by Fuji Heavy Industry LTD. Double cantilever beam test, compression after impact (CAI) test, open hole compression (OHC) test, and double notch sear strength (DNS) test were conducted for CF stitched CFRP laminates on various stitch parameters (space and pitch). Ultrasonic C-scan investigations were also conducted for measurements of impact damage size and final fracture damage size for CAI and OHC specimens. It suggested that the CF stitching to CFRP laminates affects an arresting capability of damage propagation against dynamic impact. It was also found that stitched and unstitched specimens are different in delamination propagations of final fracture mode and CAI strengths. Moreover, it is found that OHC strengths of stitched CFRP laminates improved about 10% and that final fracture damage size is smaller than unstitched specimens in the 0.111 /mm^2 (3x3) stitch density case. However, the OHC strengths of other stitch densities are not improved and the clear relationships between OHC strengths and stitch densities can not be obtained from these test results. In the DNS test, it was determined that the stitching does not affect the shear strength.

1 Introduction

Composite materials, especially CF/epoxy 2-D laminates, have the capability of light weight design for in-plane high loading structures. On the other hand, interlaminar strength is not strong against a through-the-thickness direction load (laminate peeling to out-of-plane). In some aircraft structural designs, weaknesses in the CFRP properties are critical and compression after impact (CAI), open hole compression (OHC), or resistance of interlaminar peel load such as interface of skin-stringer structure caused by buckled skin panels are typical examples. For these reasons, improvements in the CFRP's interlaminar strength gives a possibility for more light weight structures controlled by damage tolerance or post buckling design. Through-the-thickness characteristic improvements in CFRP laminates for aircraft structures by employing stitching and 3-D fabric with low cost consolidation technique such as RTM (resin transfer molding) and RFI (resin film infusion) are evaluated in the US and other countries. The authors' group carried out an evaluation of Kevlar-stitched CFRP specimens by RTM processes including static strength [1], CAI [2], fatigue[3], and fracture toughness of G_I and G_{II}[4].

In this paper, double cantilever beam (DCB), compression after impact (CAI), open hole compression (OHC), and double notch shear (DNS) strength tests for the CF stitched CFRP laminates in various stitch densities including unstitched CFRP laminates are carried out. Ultrasonic C-scan investigations are also conducted and damage size in these test specimens after impacts and after strength tests are evaluated. Moreover, sectional cut observations are conducted for fractured test specimens for various stitch parameters.

2 Experimental

2.1 Preparation of Test Specimens

The raw material of the CFRP laminates employed here are: Fiber; T700GC-12K (Toray Industries, Inc.), Resin; two parts epoxy system TR-A31 (Toray Industries, Inc.). Through-the-thickness CF thread was selected as TR-40-1K (Mitubishi Rayon Co. Ltd.). Through-the-thickness stitch threads in the laminates are schematically illustrated in Fig. 1. In this stitching method, appearances of stitch lines of each the upper and lower surface are crossed perpendicularly such as Fig. 1 (a) and (b). A picture of sectional cut of the CFRP laminates on the stitch threads is shown in Fig. 2. The present stitch is similar to the modified lock stitch in that the point where upper and lower threads connect exists on the preform surface.

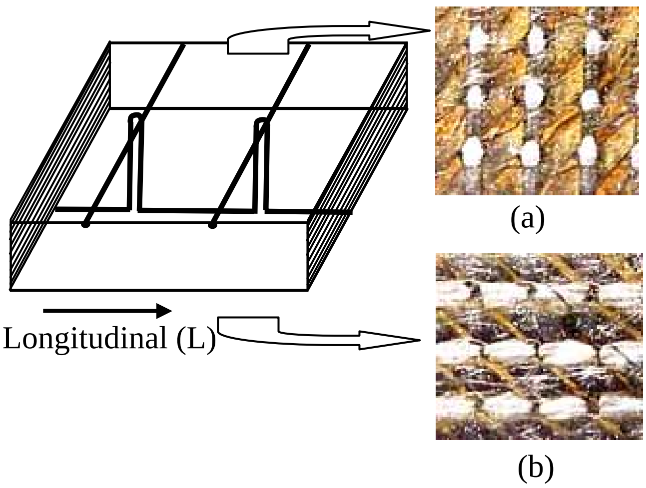

Fig.1. Through-the-thickness fiber in CFRP laminates
(a) Upper surface view (b) Lower surface view

The stacking sequence of the preform is $[45/0/-45/90]_{3S}$: quasi-isotropic. The CFRP laminates fiber coordinate system is selected so that the longitude of preform coincides with the 0° direction. The preform was inserted in the closed mold, resin was transferred into the mold, and was cured at 180°C for two hours.

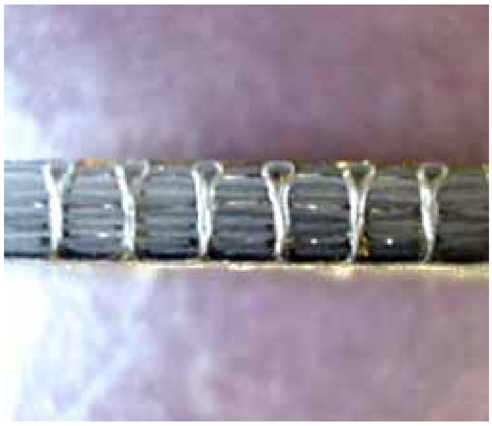

Fig. 2. A picture of sectional cut of the stitched CFRP laminates

The mother plate size is 535 mm x 300 mm. Four cases of nominal stitch parameters, 6x12, 6x6, 6x3 and 3x3 (mm x mm) are employed here. These stitch densities are 0.014, 0.028, 0.056 and 0.111 ($/mm^2$), respectively. Unstitched CFRP laminates are also prepared. The nominal thickness of CFRP laminates is 4.31 mm (24 plys). The CFRP laminates are manufactured by Fuji Heavy Industry Ltd. (FHI). Various stitch parameters of DCB, CAI, OHC, and DNS test specimens are cut from each stitched mother plate. When longitudinal directions of test specimens are in the same direction as that of the mother plate, these test specimens are referred as L series. In the same way, when longitudinal directions of test specimens are in the transverse direction of the mother plate, these test specimens are referred as T series. Therefore, L series test specimens have the same fiber stacking sequence as the longitudinal of the mother plate. T series specimens are changed into 90° in the stacking sequence of L series specimens.

2.2 DCB test

Figure 3 illustrates the geometry of the DCB test specimen employed here. Stitched DCB specimens require high bending strength caused by a high peel loading when a crack propagates. Hence, unidirectional CFRP tabs are bonded to the top and bottom of the DCB specimen. These tabs can relieve bending stress and avoid DCB specimen arms to fail before the crack propagation.

Figure 4 shows a picture of a double cantilever beam (DCB) test for a CF stitched laminate. Several broken of CF stitch threads are observed. The DCB test result is shown in Fig. 5 as relationships between interlaminar fracture toughness (G_{IR}) and volume fraction of stitch thread (V_{ft}). Three types of Kevlar stitch thickness data (111, 80, 60 tex) are superimposed on this graph. It is found that CF stitched laminates have higher G_I values than Kevlar stitched laminates at the same V_{ft}. It is suggested that CF stitched laminates show more effectiveness in G_I increase rate than the same V_{ft} of Kevlar stitched laminates.

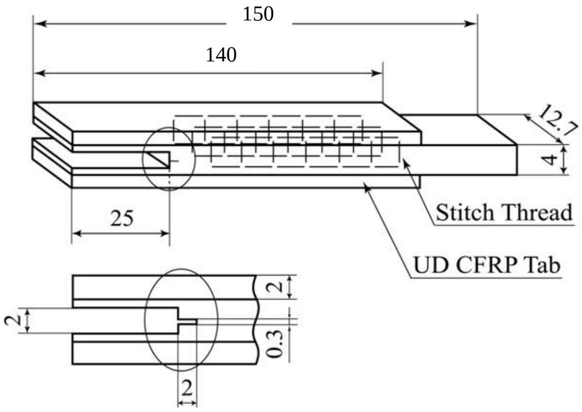

Fig.3. Geometry of DCB specimen

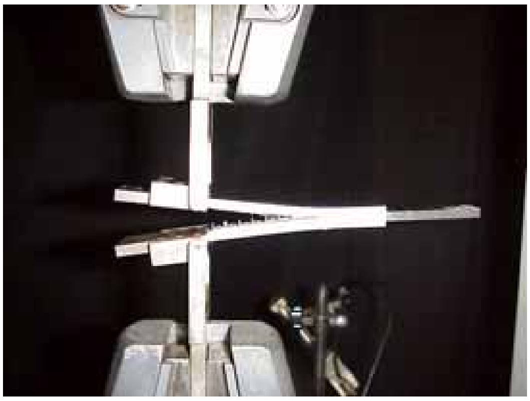

Fig.4. A picture of DCB test

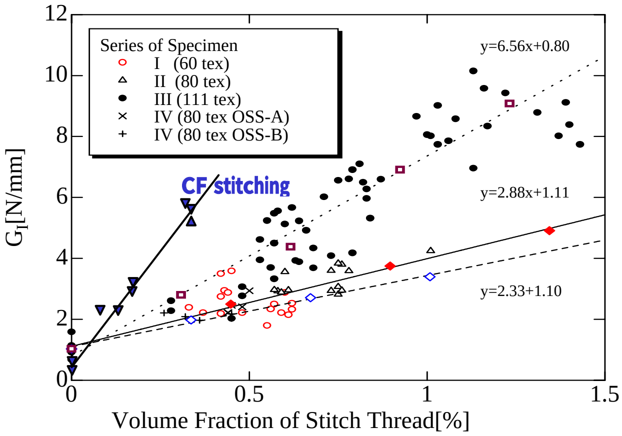

Fig. 5. Relationships between G_I and V_{ft}

2.3 CAI test

CAI test methods selected here are the JIS-R method [6] (Reference in Japan Industrial Standard) and Half-SACMA (H-SACMA) method [7]. The size of the JIS-R method is 50 mm x 80 mm x 4-5 mm and the H-SACMA method is 76 mm x 102 mm x 4-5 mm respectively. The test specimen of JIS-R method is a smaller specimen than NASA and SACMA SRM 2R methods. Therefore, their methods were proposed as a low cost test standard. However, Ishikawa [7] pointed out that there was strong possibility of obtaining poor CAI data which is caused by the occurrence of impact delamination saturation by the circular window of impact support fixture, even at a low impact energy level. This finding is considered here and the maximum impact energy level of JIS-R specimens are limited to 10.7 J (2.48 J/mm) for unstitched specimens and 3x3 stitched specimens, 5.34 J (1.25 J/mm) for the other stitched specimens.

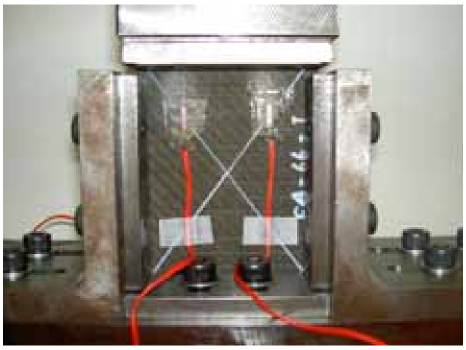

Fig.6. A picture of H-SACMA CAI test

Table 1. Test matrix of CAI strength

TEST SPEC.	Specimen Size mm	Direction	Stitch Parameter mm X mm	Stitch Density /mm^2	Energy Level (J) 0	2.67	5.34	10.7
JIS R	50×80	L&T	-	0	✓	✓	✓	✓
			6x12	0.014	✓	✓	✓	
			6x6	0.024	✓	✓	✓	
			6x3	0.056	✓	✓	✓	
			3x3	0.112	✓	✓	✓	✓
Half-SACMA	76×102	L&T	-	0			✓	✓
			6x12	0.014			✓	✓
			6x6	0.024			✓	✓
			3x3	0.112			✓	✓

Impact energy levels of H-SACMA specimens of 5.34 J and 10.7 J are selected. The impact energy levels of test specimens, stitch parameters, and CAI test specimen sizes are shown in Table 1.

The Dynamic impact devise, INSTRON /DYNATAP GRC-9250HV, is employed. All specimens after dynamic impact are examined by an ultrasonic C-scanner to measure damage size. KRAUTKRAMER SDS 5400R is used in this study. Figure 6 shows a picture of a compression after impact strength test when a CAI specimen is set up in the loading fixture. INSTRON 4500R/1128 screw driven testing machine was used. The testing speed was selected as 1.0 mm/min. These specimens, after CAI strength tests, were examined again by ultrasonic C-scanner to measure delamination damage size.

2.3.1 Test results and Discussions

Typical C-Scanning images of unstitched and stitched specimens after impact (before compression test) are shown in Fig. 7 (a) and (b) for JIS-R specimens. Both of specimens were applied as the same impact energy of 10.7 J. It is clear that the impact damage size of the 3x3 stitched specimen is smaller than the unstitched specimen. Figure 8 shows relationships between projected damage area and impact energy levels for various stitch densities of JIS-R specimens. As shown in Fig. 8, impact energy level increases with increasing damage area for all specimens. It is found that the increase rate in damage area versus impact energy curve of unstitched specimens is higher than that of stitched specimens.

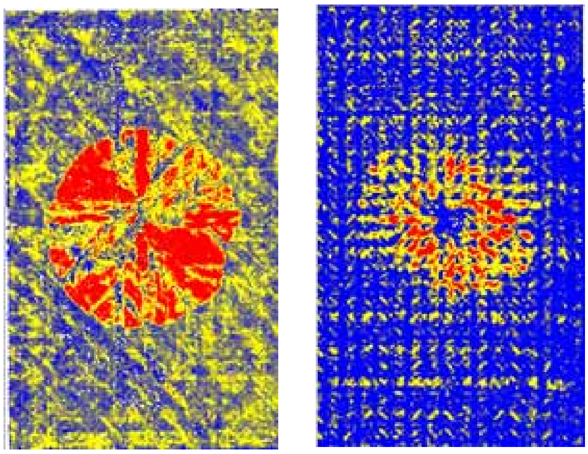

(a) (b)

Fig. 7. C-Scanning images of JIS-R specimen after impact as 10.7 J
(a) Unstitch (b) 3X3(0.111) stitched

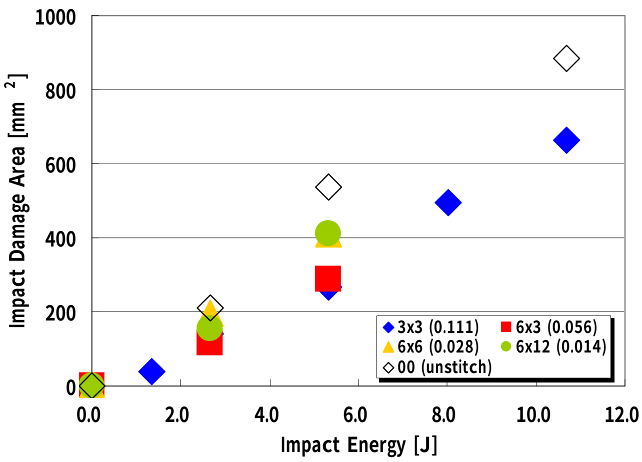

Fig. 8. Relationships between impact damage area and Impact energy levels

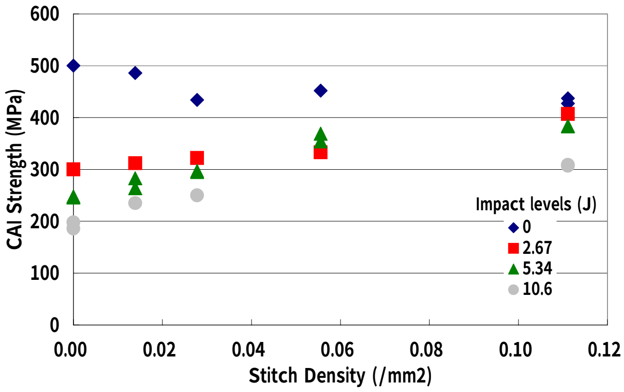

Fig. 9. Relationships between stitch density and CAI strength

Another finding is that a higher stitch density makes a smaller impact damage size at the same impact energy level. It is suggested that the CF stitching to CFRP laminates affects an arrest of damage propagation against a dynamic impact.

CAI strength and stitch density plots are shown in Fig. 9. This graph indicates that stitch density increases with decreasing compression strength for the no-impact case (zero impact energy level). The compression strength of the 0.111 (3x3) stitched no-impact specimen is lower than the unstitched specimen by about 10%. However, when impact damage exists, stitch density clearly increases with increasing compression strength.

The compression after impact strength of 10.6 J for the 3x3 stitched specimen is almost 1.5 times as high as the unstitched specimen. It is obtained from these experimental data that CF stitching to CFRP laminates affects CAI strength improvement.

Figure 10 (a) and (b) show C-scanning results on 5.34 J impact energy levels for unstitched and 3x3 stitched JIS-R specimens after CAI strength tests. There is an obvious difference in the C-scanning image of the unstitched and 3x3 stitched specimen. The image of the unstitched specimen has a large fracture damage area and must be propagated interlaminar separations, compared with the 3x3 stitched specimen. The fracture damage area of the unstitched specimen is large and expands to compression loading direction. On the other hand, the fracture damage area of the 3x3 stitched specimen is small and arrested on through-the-thickness threads positions.

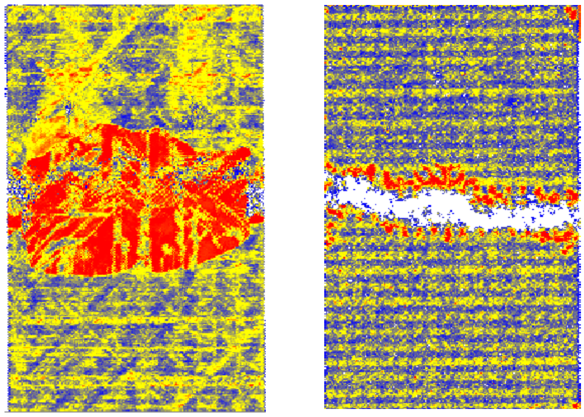

(a) (b)

Fig. 10. Fracture damage in JIS-R specimen after CAI strength test. (5.34 J)
(a) Unstitched (b) 3x3 stitched specimen

The normalized fracture damage area after strength tests to the test specimen area versus various stitch densities for JIS-R are demonstrated in Fig. 11. CAI strengths are superimposed on this graph. It is clarified that the normalized fracture damage area decreases and CAI strength increases with increasing stitch densities. It is suggested that fracture damage size of specimen after compression test is arrested and CAI strength is improved by CF stitching.

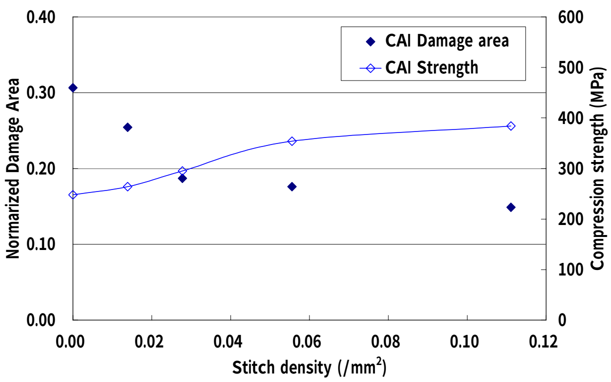

Fig. 11. Relationships between Normalized damage area or CAI strength and stitch density.

Figure 12 (a) and (d) show pictures of a sectional cut view for JIS-R and H-SACMA test specimens after strength tests. Figure 12 (a) is the JIS-R unstitched specimen and Fig. 12 (b) is the 3x3 stitched specimen. The applied impact energy level for each specimen is the same 5.34 J. The test specimens are cut along the loading direction through the middle in order to include the center of the impact position.

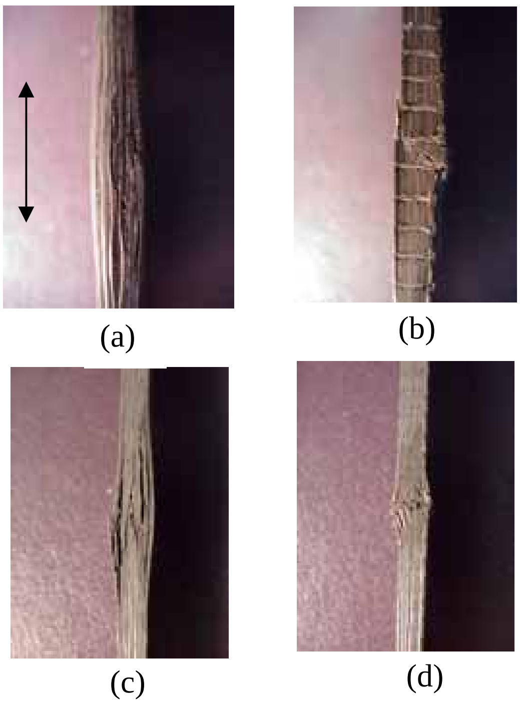

Fig. 12. Pictures of sectional cut for various stitch parameters
(a) Unstitched for JIS-R (b) 3x3 stitch for JIS-R (c) Unstitched for H-SACMA (d) 3x3 stitch for H-SACMA

It is observed that interlaminar delaminations are propagated to the loading direction in the unstitched specimen obviously, as shown in Fig. 12 (a). In the 3x3 stitched specimen, Fig. 12 (b), interlaminar delamination is partial and the appearance of fracture mode is compression, such as local buckling on inter-stitched distance. Fracture damage size of the stitched CFRP laminates after strength test is smaller than that of the unstitched specimen. Figure 12(c) and (d) show pictures of sectional cut views for H-SACMA specimens after compression strength tests of the unstitched specimen and of the 3x3 stitched specimen. The position of the section is at the center of the specimen along the loading direction where it includes the impact position. It is also observed that interlaminar delaminations occurred and propagated to the loading direction in the unstitched specimen, as the same as JIS-R specimen. On the other hand, the 3x3 stitched specimen of interlaminer delaminations are not propagated to the loading direction, as the same as JIS-R sectional cut observations results, as Fig. 12(b). It is indicated that CF stitching affects the final fracture mode of CAI test despite the different test sizes of JIS-R and H-SACMA specimens. It is also assumed that the final fracture mode of CAI strength test is changed by carbon fiber stitching.

2.4 Open hole compression (OHC) test

The NAL-III [8] method was selected as the OHC test standard. The NAL-III method is a strong candidate of a JIS standard in a draft by the JIS CFRP test standard committee. The dimensions of the test specimen is shown in Fig. 13 with stitch conditions. This specimen width and hole diameter size are the same as the SACMA SRM-3 R-94 standard, i.e., 38.1 mm and 6.35 mm, respectively. However, the length of the specimen is shorter than a SACMA specimen as 118 mm. This is an advantage of NAL-III method that the specimen size reduction effect to the cost for production of the test specimen and OHT test efficiency must be improved by the employment of small loading fixture. A picture of the OHC test is shown in Fig. 14. The OHC test speed is selected to be 1.0 mm/min. The specimen after OHC test was examined by a C-scanner for the measurement of fracture damage size.

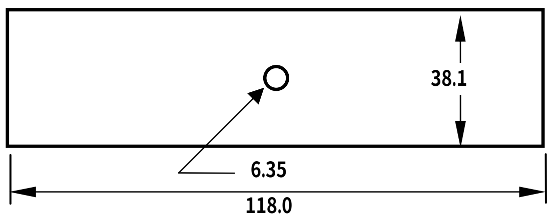

Direction	Stitch Parameter mm X mm	Stitch Density /mm^2
L&T	-	0
	6x12	0.014
	6x6	0.024
	6x3	0.056
	3x3	0.112

Fig. 13. Dimensions of NAL-III test specimen and stitch conditions

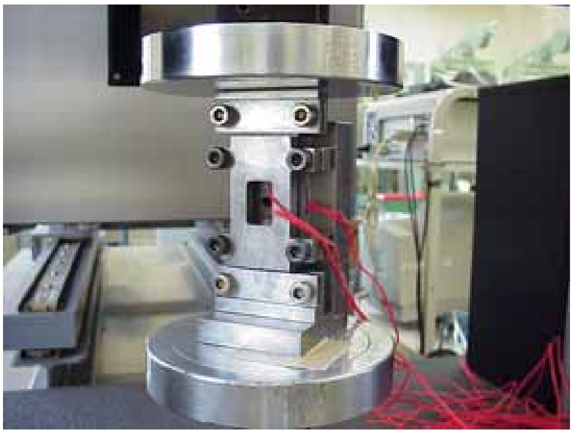

Fig. 14. A picture of NAL-III OHC test set

2.4.1 Test results and discussions

Figure 15 shows the results of OHC strength for each stitch parameter. Each test result is taken an average of 4 specimens. There is no noticeable difference for L and T series in OHC strength. The relationships between OHC strength and stitch densities are shown in Fig. 15. The stitch density 0.014 (12x6), 0.028 (6x6), 0.056(6x3) (/mm^2) are not remarkable improvements in OHC strength of unstitched CFRP laminates. However, about a 10% higher OHC strength is obtained in the stitch density 0.111 (3x3) case.

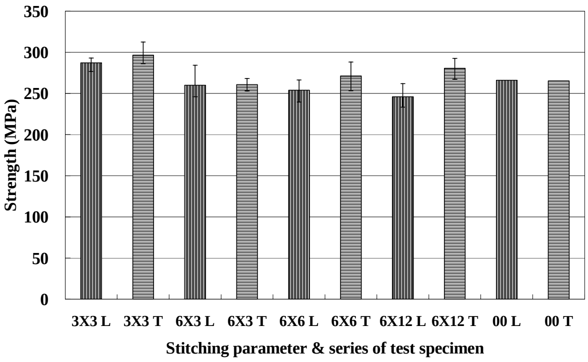

Fig. 15. OHC strength test results for various stitch parameters

The C-scanning images of the OHC test specimen after compression test are shown in Fig. 16 (a) and (b) for unstitched and 3x3 stitched specimen, respectively. It is a clear finding that fracture damage areas of unstitched OHC specimens are larger than that of 3x3 stitched specimens. Figure 17 shows relationships between damage area and OHC strength for various stitch densities. It is found that the 3x3 stitched specimen gives the smallest damage area and the highest OHC strength of all the stitch densities. However, damage area does not only show considerable scatter in the stitch density range of 0 to 0.056 /mm^2 but also OHC strength at the same level.

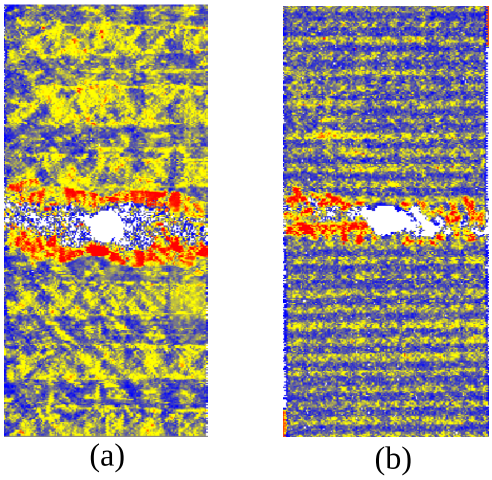

Fig. 16. C-scanning results for unstitch and 3x3 (0.111) stitched specimen after OHC test
(a) Unstitch (b) 3x3 stitched specimen

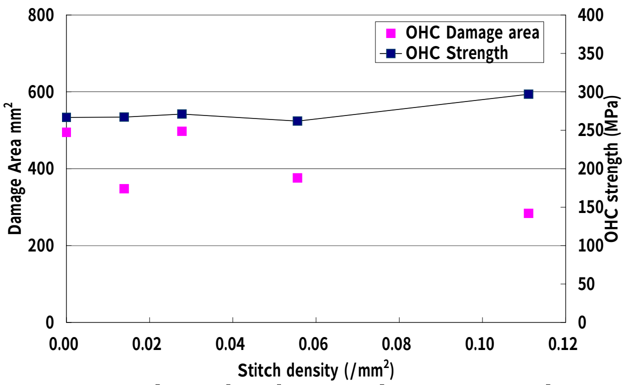

Fig. 17. Relationships between damage area and OHC strength for various stitch densities

Pictures of side views of test specimens after OHC tests for unstitched and 3x3 stitched specimens are shown in Fig. 18 (a) and (b). It is observed that interlaminar delaminations are propagated to the longitudinal direction of the unstitch specimen. On the other hand, interlaminar delaminations are not propagated to the longitudinal direction of the 3x3 stitched specimen.

As noted, it is indicated that 3x3 CF stitching to CFRP laminates affects the OHC strength improvement. However, the clear relationships between OHC strengths and stitch densities are not obtained in the present test results.

Fig. 18. Pictures of side views of OHC specimen after compression test
(a) unstitched (b) 3x3 stitched specimen

2.5 Double notch shear (DNS) test

Double notch shear (DNS) tests are conducted for various CF stitched laminates. The geometry of a DNS test specimen is shown Fig. 19, the NAL-proposed method for textile through-the-thickness composites. Double notches, one on each opposite face of the specimen and 6.4 mm apart, are sawed across the entire width of the specimen and centrally located along its length. The width of the notch is 1.0 mm and depth is half of the specimen thickness which is about 2.07 mm. The DNS tests were conducted in the L and T directions and stitch densities are 0, 12x 6, 6x6, and 3x3.

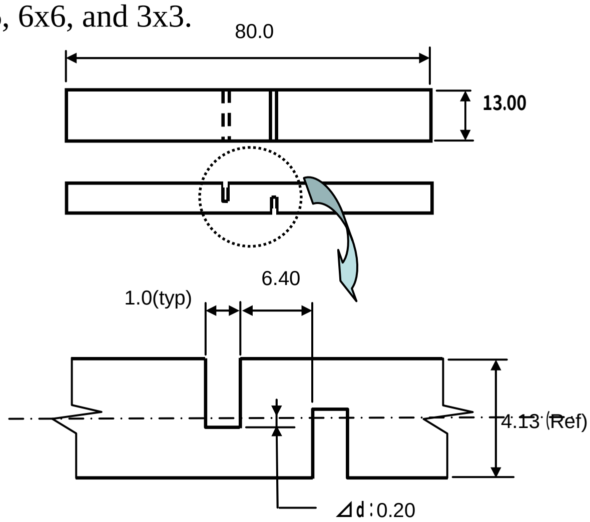

Fig. 19. Geometry of DNS test specimen

Figure 20 shows a picture of the DNS test when a DNS test specimen is inserted in the JIS K 7060A compression strength test fixture. Each DNS test specimen side is painted by white marker for clearer observation of the fracture mode. Test speed is taken as 1.0 mm/min, and the displacement of the cross-head and load curves are measured.

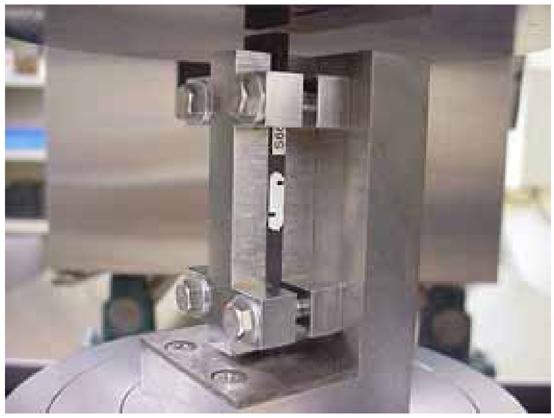

Fig. 20. Inserted in the test fixture for DNS strength test

DNS strength test results for various stitch parameters are shown in Fig. 21. An obvious difference in strengths for various stitch densities is not obtained in these test results. However, the L series strength is higher than that of the T series by about 15 %.

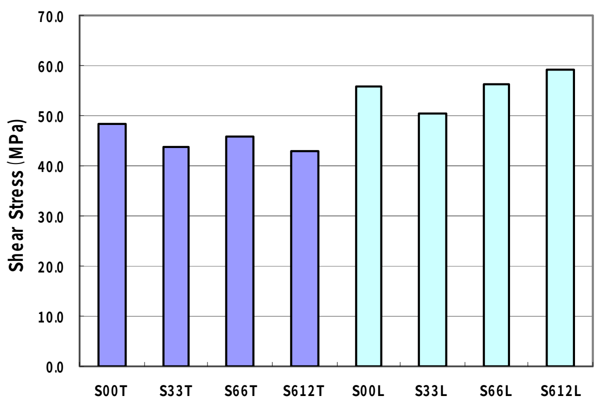

Fig. 21. DNS strength test results for various stitch parameters

A side view of a broken DNS test specimen is shown as Fig. 22, L (a) and T (b) series, respectively. The L series fractured slit is indentation shape. On the other hand, the T series slit is sharp and looks like it is along the 0 deg ply between two notches.

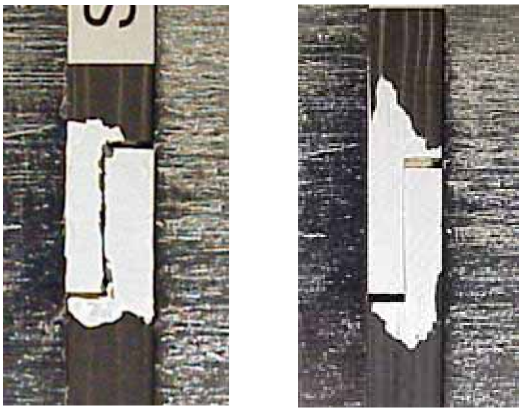

Fig.22. Fractured DNS test specimens

After the DNS test, the number of CF threads in the fractured surface is counted. A relationship between the number of stitch threads and shear strength are shown as Fig. 23. Slight degradation in shear strength is observed as the number of stitch threads increase. However, there is no clear relationship between the number of stitch threads and their shear strengths. It is resulted that CF stitching does not affect the shear strength improvement.

Fig.23. Shear strength-Number of CF threads plots

3 CONCLUSIONS

Double cantilever beam (DCB) test, compression after impact (CAI) test, open hole compression (OHC) test, and Double notch shear (DNS) test were conducted for carbon fiber stitched CFRP laminates with various stitch parameters (space and pitch). C-scanning investigations were also carried out for the measurement of impact damage size and final fracture damage size for the CAI and OHC test. The following conclusions were derived.

1) CF stitching causes on G_{IR} improvement more so than V_{ft} Kevlar stitching.
2) The carbon fiber stitching to CFRP laminates affects an arresting capability of the damage propagation against dynamic impact.
3) The compression strength of 3x3 stitched without impact specimen is lower than an unstitched specimen by about 10%. However, increasing stitch density raises compression strength. The compression after impact strength of 10.7 J for the 3x3 stitched specimen is almost 1.5 times higher than that of the unstitched specimen.
4) Normalized fracture damage area decreases and CAI strength increases with increasing stitch densities. It is suggested that fracture damage propagation of after CAI test is arrested and CAI strength is improved by CF stitching.
5) A change in final fracture mode is observed in both stitched JIS-R and H-SACMA specimens even in different sizes of specimens. Fracture delaminations propagate to the loading direction of the test specimen in an unstitched specimen. On the other hand, 3x3 stitched fractures are not propagated and are similar to the compression fracture mode inter-stitched distance.
6) 3x3 CF stitching to CFRP laminates affected the OHC strength improvement by about 10%. However, the clear relationships between OHC strengths and stitch densities could not be obtained in the present work.
7) CF stitching does not affect shear strength improvement.

Acknowledgement

This work has been supported by NEDO (New Energy and Industrial Technology Development Organization) and JADC (Japan Aircraft Development Corporation) under the control of METI of the Japanese government. The authors also would like to express gratitude to Mr. Fujishima, Mr. Yamazaki and Mr. Ichikawa in Ishikawajima Jet Service Co., Ltd who supported many tests, and Mr. Shin Horikawa, Mr. Masataka Yamamoto, Mr. Hiroyuki Akiyama, and Mr. Taichi Itabashi who carried out the DCB, CAI, and OHC tests.

References

[1] Y.Tada and T.Ishikawa, *Key Engineering Materials*, vol.37, (1989), pp.305-316.

[2] Y.Tada and M.Matusima et al, *Proc. 19th Symposium on Composite Materials*, (1994), pp.57-60.

[3] Y.Iwahori and T.Ishikawa et al, *Proc. 9th US-Japan Conference on composite Materials*, pp.761-768.

[4] S.Horikawa and Y.Iwahori et al, *Proc. 8th Janap International SAMPE Symposium*, (2003), pp509-512.

[5] T.Ishikawa and Y.Iwahori, *Proc. 48th International SAMPE Symposium*, (2003), pp.779-792.

[6] Association for Japan Industrial Standard, *JIS K-7089-1996*, (1996).

[7] T.Ishikawa and M.Matsushima, *Proc. 9th US-Japan Conference on composite Materials*, (2000), pp.133-140.

[8] Y.Hamaguchi and Ishikawa et al, Proc. of JSMS Composites 33, (2004), pp.65-66.